Journal of Autonomous Intelligence (2023) Volume 6 Issue 3
doi: 10.32629/jai.v6i3.789

ORIGINAL RESEARCH ARTICLE

Future fusion+: Breast cancer tissue identification and early detection of deep hybrid featured based healthcare system

Shruthishree Surendrarao Honnahalli[1,*], Harshvardhan Tiwari[2], Devaraj Verma Chitragar[1]

[1] *Department of Computer Science and Engineering, Faculty of Engineering and Technology, JAIN (Deemed-to-Be University), Jain Global Campus, Jakkasandra, Kanakapura Road, Harohalli, Ramanagara District, Karnataka 562112, India*

[2] *Techschool, New Zealand Skills and Education Group, Auckland 1010, New Zealand*

*** Corresponding author:** Shruthishree Surendrarao Honnahalli, sh.shruthi@jainuniversity.ac.in

ABSTRACT

The exponential increase in cancer cases, particularly breast cancer (BC), has prompted academics and business to develop more effective and trustworthy methods for classifying and identifying BC tissues. In contrast to traditional machine learning (ML) techniques, this work presents the development of a fusion of features AlexResNet+: a deep hybrid feature-based system of early BC detection in healthcare tissue identification. For deep feature extraction, we employed three of the most popular and effective deep learning models, AlexNet, ResNet50 and ResNet101. We employed ResNet50 with modified layered architectures while using AlexNet with five convolutional layers in order to maintain high dimensional deep features while maintaining the best computational efficiency. As a result of combining the deep features from the AlexNet and ResNet DL models, we were able to perform two-class classification using the Support Vector Machine with Radial Basis Function (SVM-RBF). Performances for AlexNet, shorted ResNet50, and hybrid features were collected separately to evaluate the effectiveness of the various feature sets. The counseled hybrid deep capabilities (AlexResNet+)-primarily based version has a most class accuracy of 95.87%, precision of 0.9760, sensitivity of 1.0, specificity of 0.9621, F-Measure of 0.9878 and AUC of 0.960, according to simulation results using DDMS mammography breast cancer tissue pictures.

Keywords: deep learning; feature fusion; AlexNet; ResNet; computer-aided diagnosis (CAD); residual network (ResNet); concatenated feature vector (CFV); breast cancer diagnosis; breast cancer tissue categorization

ARTICLE INFO

Received: 26 June 2023
Accepted: 19 July 2023
Available online: 15 September 2023

1. Introduction

The second-main purpose of most cancers-associated deaths among women these days is BC. According to the World Health Organisation (WHO), 17.1 million cases of advanced cancer were discovered worldwide in 2018. By 2040, there will be 16.3 million cancer-related deaths and 27.5 million new cases of cancer, according to the World Health Organisation (WHO). Mammography can identify breast cancer early. This is often achieved by looking for different hundreds and/or microcalcifications in specific loads; as a result, the detection and classification techniques are frequently less accurate. This is due to the same properties they share. A convolutional neural network (CNN) and its variants, one of the most well-liked deep learning models, have been utilised in a number of medical image processing applications. The symptoms are shown in **Figure 1**.

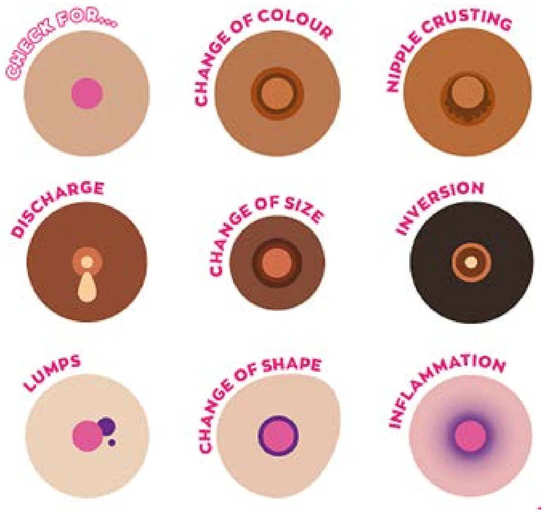

Figure 1. Symptoms for breast cancer.

Several symptoms of breast cancer include:

- A change in the breast's size, shape, or appearance.
- A growth or bulge in the underarm or breast area.
- Both an inversion and a rippling discharge.
- On the breast, there are visible skin changes, including redness, dimpling, or puckering.
- A hurt or achy breast.
- A lump or growth under the arm.
- An obvious difference between the breasts.
- Large or lumpy lymph nodes under the arm.

Although not all breast lumps or changes are indicative of breast cancer, it's still crucial to have them examined by a medical practitioner to rule out any other potential problems. As advised by their doctor, women should also undertake monthly self-exams and undergo routine breast exams.

Today, early detection of breast cancer is more crucial than ever because it can greatly enhance the effectiveness of treatment. Medical imaging has undergone considerable changes as a result of technological and scientific advances, including mammography, the gold standard for the early identification of breast cancer. In order to increase the precision and effectiveness of mammographic detection, deep learning models, such as those built on the ResNet and AlexNet architectures, have shown promise. They may also be used to predict breast cancer in its early stages. These algorithms may reliably identify the presence or absence of breast cancer at an early stage by analysing mammograms and other imaging data, allowing for prompt interventions and therapies. Additionally, risk assessment models that can pinpoint women who have a higher risk of developing breast cancer are receiving more attention, enabling targeted screening and prevention methods[1].

Using deep learning approaches, histopathological image categorization can be done for diagnostic purposes by extracting (deep) features. There is little doubt that the bulk of machine learning and deep learning techniques now in use have been surpassed by deep learning techniques like ResNet and AlexNet. Their efficiency becomes more honed as a result of their independence from other feature extractors[2]. The cancer cells are shown in **Figure 2**.

Based on the gene expression profile, **Figure 3** shows several molecular subtypes of ductal breast cancer that can be identified. Regarding their immunological microenvironment, which comprises the kinds and numbers of immune cells present in the tumour, these molecular subtypes have diverse properties.

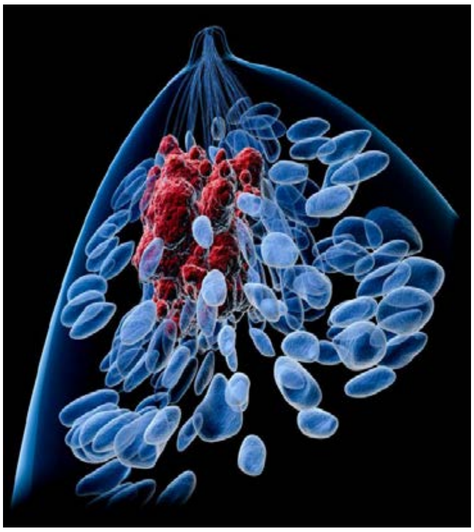

Figure 2. Cancer cells in breast.

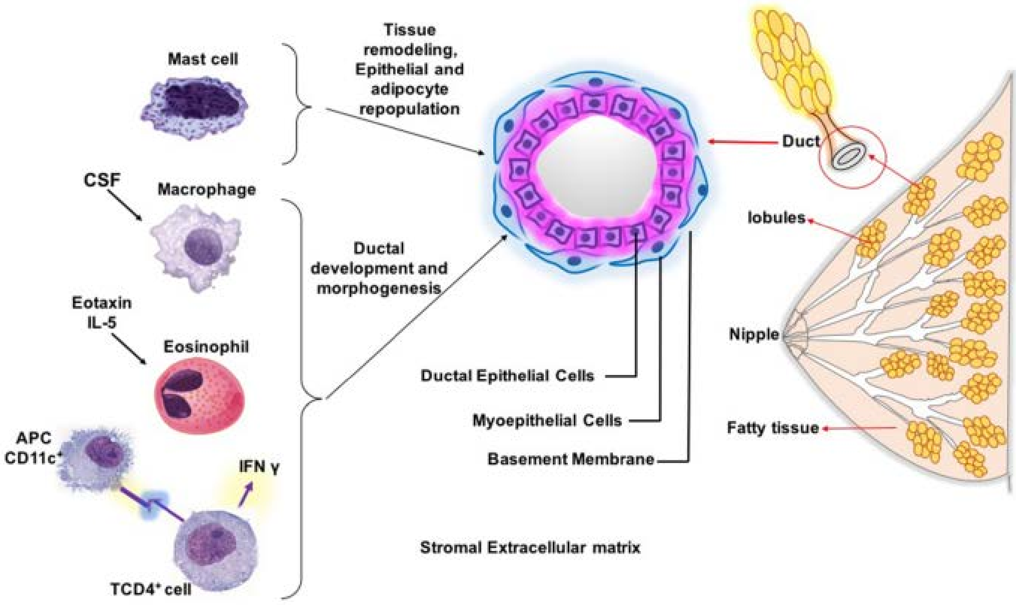

Figure 3. Various immune microenvironment subtypes are associated with ductal breast cancer.

These models estimate a woman's chance of getting breast cancer using a variety of variables, including age, family history, lifestyle factors, genetic markers, and others. Overall, research into early breast cancer prediction is advancing quickly, and deep learning models like AlexNet and ResNet are essential to enhancing the precision and effectiveness of breast cancer screening and diagnosis. It is probable that we will see further improvement in this area with continuous study and technological breakthroughs, improving outcomes for breast cancer patients[3–6].

The effective breast cancer therapy and management depend on early detection of the illness. The AlexNet and ResNet architectures, among other deep learning models, have shown potential for enhancing the precision and effectiveness of mammographic detection and can also be utilised for breast cancer early detection. A pre-trained model may be used as a starting point to build an early prediction model for breast cancer using AlexNet and ResNet. Pretrained models are deep learning models that may be improved on a smaller dataset for a particular task after being trained on a big dataset, such as ImageNet. With the intention of identifying breast cancer in its earliest stages, when it is most curable, early-stage mammographic detection is a significant field of research in medical imaging. Deep learning models are becoming more and more popular as a way to boost mammogram detection's precision and effectiveness[6].

Using a mix of several architectures is one way to enhance the performance of these models. For enhancing mammographic detection, the AlexNet and ResNet architectural combinations have particularly shown potential. The combination of bots AlexNet and ResNet101 is defined as a fusion of features (AlexResNet+). One of the first deep learning models to perform at the cutting edge on the ImageNet dataset was the convolutional neural network (CNN), AlexNet. It consists of many convolutional layers followed by fully linked layers and has been shown to be effective in photo categorization tasks. The more modern ResNet architecture addresses the issue of fading gradients in very deep neural networks. In order to enable the network to learn residual mappings and avoid performance loss as the network depth rises, it employs skip connections[7].

Here are the steps that can be taken to use ResNet and AlexNet to develop a breast cancer early prediction model:

- Gathering and preparing data assemble a database of mammograms with labels identifying the patient's breast cancer status. Make sure the photos have been preprocessed so they are in a format that the model can learn from.
- Picking a trained model: pick an AlexNet or ResNet model that has been trained.
- Transfer learning: on the basis of the mammography dataset, fine-tune the pretrained models as a starting point. This entails freezing the model's initial layers, which learn generic picture properties, and then training the subsequent layers on the mammogram dataset to learn features unique to the purpose of predicting breast cancer.
- Evaluation of the model: assess the model's performance on a validation set. Calculating measures like accuracy, precision, and recall can be used to do this.
- Testing: To evaluate the finished model's generalisation capabilities, run it on a different test set.

Overall, combining pre-trained models from AlexNet and ResNet can be a successful strategy for breast cancer early detection. Such models have the potential to increase the precision and effectiveness of breast cancer screening and diagnosis with more study and improvement[8–10].

The two different convolutional neural network (CNN) models: ResNet50 and ResNet101.

ResNet is a deep CNN architecture that became well-known for its capacity to train extremely deep neural networks, hence the name ResNet50 (residual network-50). ResNet50 has 50 layers, as indicated by the "50" in its name. In ResNet, a notion known as residual connections is introduced, which aids in addressing the vanishing gradient issue during training. These connections enable the network to skip several levels, improving information flow and making deep network training simpler. For many computer vision tasks, such as object detection and image classification, ResNet50 has been extensively employed.

ResNet101: With 101 layers, ResNet101 is a more complex variant of ResNet50. With more layers and the same residual learning techniques, it may capture increasingly more complex features and representations. ResNet101 similarly consists of residual blocks, but each block in ResNet101 has more layers than ResNet50. ResNet101's architecture typically consists of: max-pooling is used after a convolutional layer to process the input image. There are four different sets of residual blocks, each with three, four, or 23 levels, pooling global averages to cut down on spatial dimensionality, a layer that is completely connected to provide the categorization output. ResNet101 is more complicated and, in theory, has the ability to learn more complex patterns, but it also has higher processing and memory requirements for training and inference.

2. Related work

A. Pre-processing for the MLO (mediolateral oblique) image of mammography frequently involves removing the pectoral muscle. In this view, the pectoral muscle can frequently obscure the breast tissue, making it challenging to decipher the image and possibly obscuring small lesions. The visibility of breast tissue and the reliability of mammography interpretation can both be improved by removing the pectoral muscle. Image processing software is used to locate the pectoral muscle in the image, locate it in the image, and then delete it from the image. A radiologist or technician can perform this manually, or automated software methods can be used.

The procedures for removing pectoral muscles include:

Determine where the pectoral muscle is located in the picture. Utilise image segmentation techniques to separate the pectoral muscle from the surrounding breast tissue. Remove the image's segmented pectoral muscle. Using interpolation or other methods, fill in the blanks with the surrounding breast tissue to complete the picture. It is essential to remember that not every mammogram requires or warrants the excision of the pectoral muscle. It depends on the particular patient and the chosen illustration. For accurate interpretation, it may occasionally be required to retain the pectoral muscle in the photograph. A skilled radiologist or other medical expert should decide whether to remove the pectoral muscle.

B. Image enhancement: region based method: the process of improving particular regions of interest while maintaining the visual quality of the surrounding areas is known as "region-based image enhancement." It is a form of in-camera local picture enhancement that emphasizes particular areas or details.

The following steps are involved in region-based picture enhancement:

- Determine the areas of the image that are of interest.
- Create a mask or a zone of impact that identifies the enhancement target.
- Apply the enhancing technique only to the chosen area, leaving the remainder of the image alone.
- To provide a seamless transition between the improved and unenhanced sections, blend the enhanced region with the surrounding environment.

Histogram equalization, contrast stretching, and local adaptive filtering are a few examples of region-based picture improvement methods. A common technique in area-based picture enhancement is histogram equalization, which modifies the histogram of the chosen region to provide a more uniform distribution of intensity values. This may aid in enhancing the contrast and clarity of the features in the chosen area[11].

By modifying the intensity values of the chosen area, contrast stretching can increase the contrast between the lightest and darkest pixels. This may aid in enhancing the region's overall sharpness and visibility. Applying a filter to the chosen area while taking into consideration the local picture features is known as local adaptive filtering. Within the chosen area, this might help to lessen noise and improve fine details. In medical imaging, when specific regions of interest, such as tumours or lesions, need to be emphasized for diagnosis and treatment planning, region-based image augmentation can be very helpful.

C. Segmentation: region based thresholding (region growing + region clustering) avoid FP: a common image segmentation approach called region-based thresholding divides an image into areas based on the homogeneity of pixel intensities. Two frequently used techniques in region-based thresholding are region expansion and region clustering. A seed pixel is chosen for the region-growing process, which adds successive neighbouring pixels with comparable intensities to the region. Until the entire area is planted, this process is repeated. On the other hand, region clustering is a method that creates clusters of related pixels. Usually, clustering algorithms like k-means clustering are used for this. However, if there is a lot of noise in the image or if the threshold is not set correctly, these algorithms may result in false positives (FP). Several tactics can be used to prevent these false positives[11,12].

The segmentation can be gradually refined to finer resolutions by using a multi-scale region growth technique, which starts with a coarse resolution. This method can assist in removing potentially false-positive regions. Another method for removing false positives is to use a post-processing phase. The segmented regions can then be subjected to morphological procedures like erosion and dilation, or regions can be classified as true or false positives using machine learning approaches. Finally, to prevent false positives, the threshold value must be carefully chosen. This can be accomplished by examining the pixel intensity histogram and choosing a threshold value that effectively distinguishes the object of interest from the background while reducing false positives[13,14].

D. Feature extraction: multiresolution feature: in computer vision and image processing, the multiresolution feature extraction technique is used to extract features from an image at several scales or resolutions. With this method, features are extracted from each scale or level after an image has been divided into multiple scales or levels. The wavelet transform is the method of multiresolution feature extraction that is most frequently utilised. A set of wavelet functions is used in the wavelet transform to divide a picture into various sizes or levels. With high-frequency bands containing fine features and low-frequency bands holding coarse details, each level corresponds to a particular frequency band. Then, using various methods like histogram analysis, edge detection, and texture analysis, features can be extracted from each level. The pyramid algorithm is another method for extracting features from many resolutions. The low-pass filter and image subsampling steps of the pyramid algorithm create a series of low-resolution images. Then, features from each level of the pyramid can be extracted using methods like template matching, edge detection, and blob detection[15].

E. Classification: DNN ResNet (residual N/W): the use of deep neural networks (DNNs) for image classification tasks is highly effective. The DNN architecture known as ResNet, or residual network, has attained state-of-the-art performance in image classification tasks.

ResNet's central concept is to create connections that skip over or circumvent one or more network layers. The goal of these shortcut connections is to improve the network's information flow and solve the issue of vanishing gradients, which can make it challenging to train very deep neural networks. A number of residual blocks make up the ResNet architecture, and each block has many convolutional layers followed by batch normalization and activation functions. The ResNet shortcut connections omit one or more residual blocks and combine the input with the output to form a residual or "skip" link. In order to reduce the classification error, the network learns to modify the weights of the residual blocks. As a result, the network's classification ability is enhanced as it learns intricate and abstract properties from the input photos. ResNet's ability to train very deep neural networks (up to hundreds of layers) without experiencing the issue of vanishing gradients is one benefit it has over other DNN architectures. As a result, ResNet performs at the cutting edge on the ImageNet dataset and other image classification tasks. ResNet is an effective DNN architecture for classifying images that leverages shortcut connections to speed up data transmission and solve the issue of vanishing gradients. It is a well-liked option for a variety of image classification problems due to its capacity to build incredibly deep neural networks[15–17].

3. Proposed methodology

The deep hybrid ML model for breast tissue recognition involves four steps.

Phase 1 involves the collection of data and augmenting;
Phase 2 involves extraction of features using AlexResNet+;

Phase 3 includes feature selection technique;

Phase 4 involves two-class SVM-RBF techniques.

The following sections provide a complete view of these progressive implementations.

A. The collection of data and augmenting:

In order to evaluate the performance of the suggested algorithm for the classification and categorization of breast cancer cells, it used a well-known testing dataset known as the DDSM. With an average pixel size of 3000 × 4800 and a resolution of 42 microns with 16 bits, DDSM is gathered to represent the original breast data. 43 distinct volumes were created from the 2620 breast mammography scans that make up the DDSM database. These findings demonstrate how impartial and experienced radiologists can recognise and annotate malignant tumours. A sample of the single sample data from the DDSM for pictures of benign and malignant breast cancer is shown in **Figure 4**. In order to prevent insertion biases in classification or prediction using alternative morphological procedures, we first modified mammography pictures using affine transformation for data augmentation. Patching the mammography images was the other method used for data augmentation.

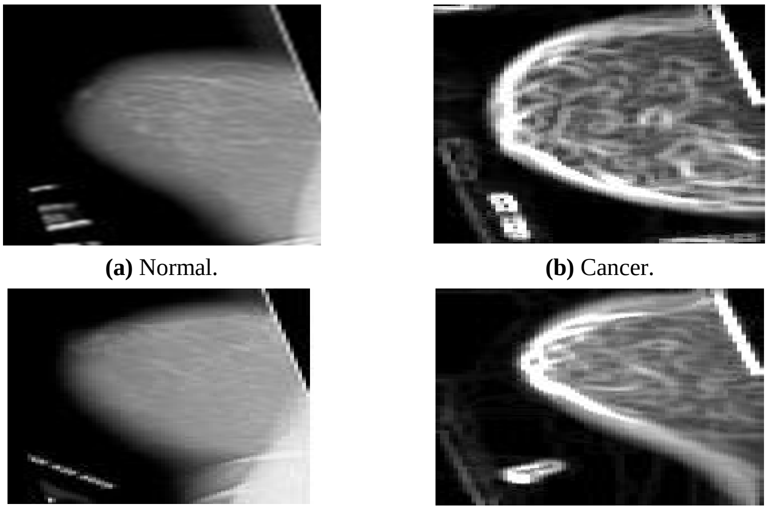

(a) Normal. **(b)** Cancer.

(c) Normal. **(d)** Cancer.

Figure 4. DDSM data samples are shown.

The effect of this technique is to isolate bits or fragments of an image that have a similar structure but come from separate groups of images. To facilitate better quantitative analysis, this involved moving all microscopic breast mass images into a common area. Here, we randomly added colours to both the benign and cancerous photos that were classified[17]. For our proposed job, each original image was down-sampled to a resolution of 1024 × 768 pixels. We also retrieved 150 × 75 pixel crops from the down-sampled images. 20 crops were used to represent each mammogram, and when it was decided that the amount of data was adequate, 20 descriptors were further used to further encode the crops. Mathematically, we use Equation (1) to obtain the single descriptor[18,19].

$$d_{\text{pool}} = (1/\mathrm{N} \sum_{i=1}^{N} (di)p)^{1/p} \quad (1)$$

We set the value of p to 3, here, N denotes the total number of crops, di denotes a crop's descriptor, and d-pool denotes the pooled descriptor of each mammogram. Notably, the p-norm of a vector allows for a maximum value of p and an average value of $p = 1$. As a result, a significant number of descriptors are produced for each original mammography image, assisting in the creation of an ideal set of features for subsequent categorization.

B. Extraction of features using AlexResNet+:

The ResNet50 deep and AlexNet CNN networks' deep features were combined for this investigation. Our main goal is to extract and employ a combination of deep (AlexNet with a 4096 kernel) and changing depth features (shorted residual ResNet50) to classify breast cancer in this case more accurately and effectively. These deep learning models are described using the information below: the deep features collected from the ResNet50 deep and AlexNet CNN networks were the main focus of this investigation. In this case, our main goal is to extract and apply a blend of deep (AlexNet inside 4096 kernels) and variable intensity data (residual ResNet50) to conduct a more effective and accurate breast cancer diagnosis. For these deep learning models, the following details are given: the first CNN framework to outperform DL techniques for categorization and item recognition was AlexNet. The pre-trained model was used to generate AlexNet CNNs, which were designed to undertake different item categorizations. Because of their adaptability, they may also be used to extract image features for breast cancer in bulk. Traditional CNN receives 256-D, but at FC levels, we get 4096-D[20,21].

a) AlexNet

The first CNN model to outperform the most popular DL models currently available for object recognition and classification is known as AlexNet. Despite the fact that AlexNet CNN was created to work with the pre-trained model to accomplish various object classification tasks, because of its robustness, it can also be effectively applied as a transferable learning model for extracting breast cancer mass picture features.

In contrast to traditional CNN, which recovers 256 dimensional features, we were able to retrieve 4096 dimensional features at the FC layers, which offers depth information to make better decisions. We used two FC layers (FC6 and FC7) in addition to five convolutional layers (CONV1, CONV2, CONV3, CONV4, and CONV5) in our suggested AlexNet CNN design. Of the three potential completely connected layers (FC6, FC7, and FC8), FC8 stood out because of its 1024-dimensional properties. Contrarily, the 4096-dimensional features in the FC6 and FC7 levels were greater than those in the FC8 layer. **Figure 5** depicts AlexNet CNN architecture[22,23].

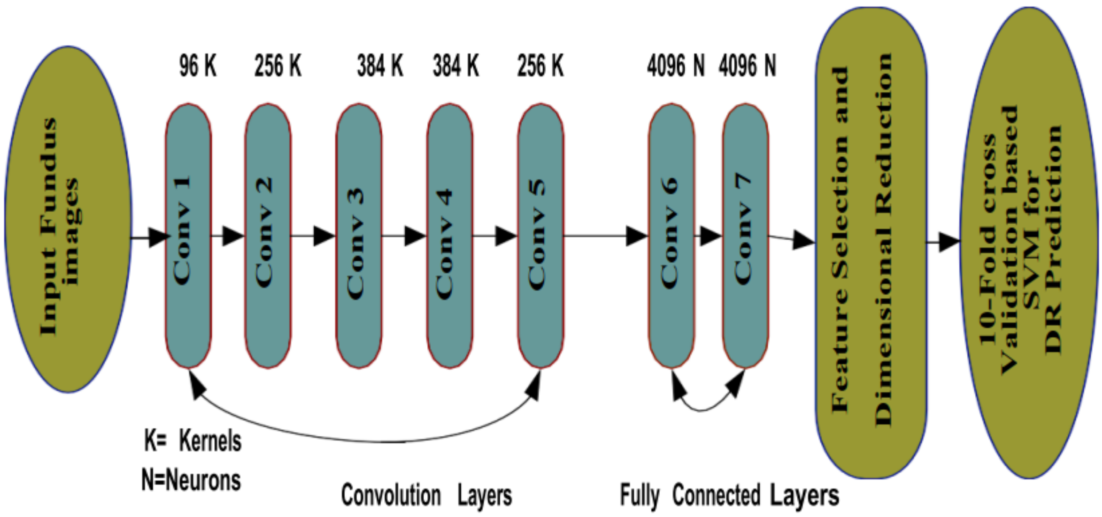

Figure 5. AlexNet CNN architecture.

Hence, we only took these characteristics into consideration for subsequent classification. In AlexNet-CNN's traditional architecture, there are eight layers total, including five convolutional layers and fully linked layers. **Figure 5** depicts the proposed AlexNet CNN's general layout. In our suggested model, the 96-neuron AlexNet (or first CONV-layer of AlexNet) was directly fed the augmented images as input. In this case, each

CONV-layer produced unique features. After being resized, the outputs underwent further processing before being sent to the following stages:

b) CONV

The vertical and horizontal filters that make up the convolutional layer—often abbreviated as CONV can combine to extract and incorporate feature patterns from the input images. The neurons or kernel specifications on the CONV layer consist of [CONV (1)-96, CONV (2)-256, CONV (3)-384, CONV (4)-386, and CONV (5)-256] kernels[22,23]. Every neuron in the current study of mammography image feature extraction for breast cancer screening generated an image representation with identical weights (WI) and bias (BI). These parameters were designed to help neurons discover similar features during feature mapping. A normalisation layer does not connect the third, fourth, or fifth levels. The fourth level has $3 \times 3 \times 384$ kernels, while the third tier's 384 kernels are $3 \times 3 \times 256$. Two FC layers, five CONV layers, and 4096-D kernels.

c) Layer of max-pooling

The main purpose of a max-pooling layer is decrease the size of the input while reserve the most important information. In a max-pooling layer, the input feature map is divided into a set of non overlapping rectangles, called pooling regions. For each pooling region, the maximum value within that region is taken as the output of the pooling operation, and that value is passed to the next layer. The pooling window size and the stride are commonly used to specify the size of the pooling regions. The pooling window size determines the size of the pooling regions, while the stride determines the distance between adjacent pooling regions. Max-pooling is typically used after convolutional layers in a CNN to progressively reduce the spatial dimensions of the feature maps and capture the most important features at multiple scales.

d) ReLU normalisation layer

Convolution was performed while using ReLU. A non linear component operator that behaves like a level is present in the ReLU layer. In our model, there are three ReLU layers. ReLU separates the neuron's y inputs and outputs. In ReLU, $q(x)$ is translated into x if x is less then 0 and into (x) if $f(x) > 0$. The outcome will specifically state that a slope multiplied by 0.01 or setting it to 0 will prevent the negative sections from occurring. We activated that 0 barrier and provided = zero to make our model behave as a ReLU characteristic with $q(x) = \max(0, x)$. There are eight layers within the AlexNet-conventional CNN, which includes 5 CNN layers and absolutely connected levels[23,24].

e) ResNet50

The residual network is yet another name for ResNet. Restructured CONV layers are included in the ResNet deep model to learn residual functions alongside the inputs. In contrast to traditional deep learning models, residual networks, particularly ResNet, are simpler to tune in order to retrieve more detailed and varied information (such features)[19]. Identity mapping is typically carried out by a "residual block (RB)" that runs in parallel with the CONV layers and is connected to each CONV in the form of a "shorted connection". Before the outcome is transferred to the following block, the output of the CONV is first added to the output of the shortcut branch. Actually, ResNet's network architecture has changed in addition to utilising the previously described "shorted connection". "VGGNet served as the basis for ResNet's network architecture". In this scenario, each CONV has tiny kernel values that measure 3 in size[24,25].

The breast's mammographic pictures were loaded into our suggested ResNet deep learning model as input, retrieving high-dimensional characteristics. We created a ResNet model with several activation functions that allowed it to simultaneously extract and learn from features from many mammographic mass pictures. Here, ResNet50 improved the input photographs or extracted numerous attributes from various viewpoints. It maintained $150 \times 75 \times 3$ dimensions through picture resizing or the use of enhanced images. Our suggested

ResNet50 demonstrated multi-layer feature extraction after training over the extracted features for each breast mammography image. We retrained the inputs to maintain higher efficiency and quick convergence[26,27].

We retrained the inputs by adding a residual block denoted by Equation (2) in order to maintain higher efficiency and quick convergence.

$$y = F(x, \{W_i\}) + x \tag{2}$$

The input and output vectors of the residual layer are represented, respectively, by the letters *x* and *y* in Equation (2) above. Here, (*x*, "*Wi*") represents the remaining mapping information between the input images that remains to be learned. **Figure 6** depicts the residual map's functional architecture. ResNet50 and a shortcut addition were used to solve the loss function, as shown, without the need for new parameters or alternate computational work.

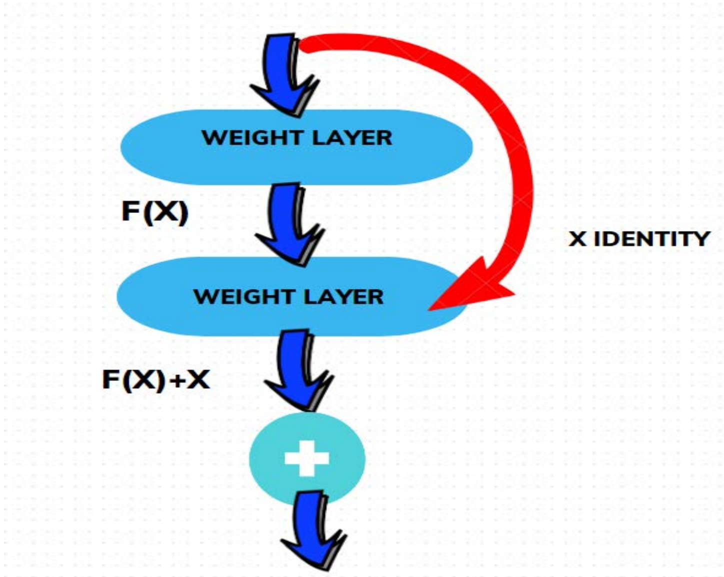

Figure 6. Identity block.

Notably, batch normalisations of the input images were done for our proposed ResNet model. In other words, we added a layer called batch normalisation on top of the three-channel layer that came before it. In this case, it normalised each input channel over a mini-batch (we utilised three channels). Between CONV and non-linearity (i.e., the ReLu layer), we used a batch normalisation layer to improve training efficiency and reduce the susceptibility to network initialization. It was able to normalise the activations of each channel by dividing the mini-batch standard deviation and eliminating the mini-batch average. The input was scaled using a learnable scale factor after being moved by a learnable offset value[28,29].

In order to keep essential characteristics while requiring less processing, we modified ResNet50. We recently obtained the final deep features for FeatResNet to be utilised for two-class classification using the SVM-RBF machine learning technique, despite the fact that typical deep learning models like AlexNet and ResNet50 employ a final dense layer with soft max activation to conduct classification. The full implementation concept of the used ResNet50 model with concealed units is shown in **Figure 5**. We merely acquired the final deep $Feat_{ResNet}$ features, which will be used with the SVM-RBF machine learning method for two-class classification.

f) ResNet101 pre-trained model description

Model ResNet, which stands for recurrent network architecture which used for the classification challenge, and it contains an essential aspect of computer vision issues. ResNet exploits residual connections that gradients may flow through to prevent chain rule zeroing. The total convolutional in ResNet101 is 104. It has

3 × 3 blocks of layers, and 29 of them use the preceding block's output data, as mentioned above. These returns are the initial parameter of the adding function utilized after every loop to recover its input. The result from the previous block is used in the next four blocks, which operate in a sequence with a sampling frequency of 1 × 1 and a take a step of 1. At the block's outputs, the summation receives the outcome. The framework of ResNet is shown in **Table 1**.

Figure 7 depicts block illustration of residual module. After preprocessing, the dataset included 2850 Glioma, 2124 Meningioma & 2745 Pituitary disease. Additionally, it was arbitrarily split into learning of test database in a 9:1 proportion. 10% of the entire dataset is testing information.

Table 1. Framework of RESNET.

Layer name	**O/p size**	**101-layers**
Convolution 1 layer	112 × 112	stride 2, 7 × 7, 64
Convolution 2 layer	56 × 56	3 × 3 maximum pooling, stride 2 $\begin{bmatrix} 1 & 164 \\ 3 & 364 \\ 1 & 1256 \end{bmatrix} \times 3$
Convolution 3 layer	28 × 28	$\begin{bmatrix} 1 & 1128 \\ 3 & 3128 \\ 1 & 1512 \end{bmatrix} \times 4$
Convolution 4 layer	14 × 14	$\begin{bmatrix} 1 & 1256 \\ 3 & 3256 \\ 1 & 11024 \end{bmatrix} \times 23$
Convolution 5 layer	7 × 7	$\begin{bmatrix} 1 & 1512 \\ 3 & 3512 \\ 1 & 12048 \end{bmatrix} \times 3$
	1 × 1	Regular pool,1000-D fc, soft max
FLOPs	-	7.6 × 109

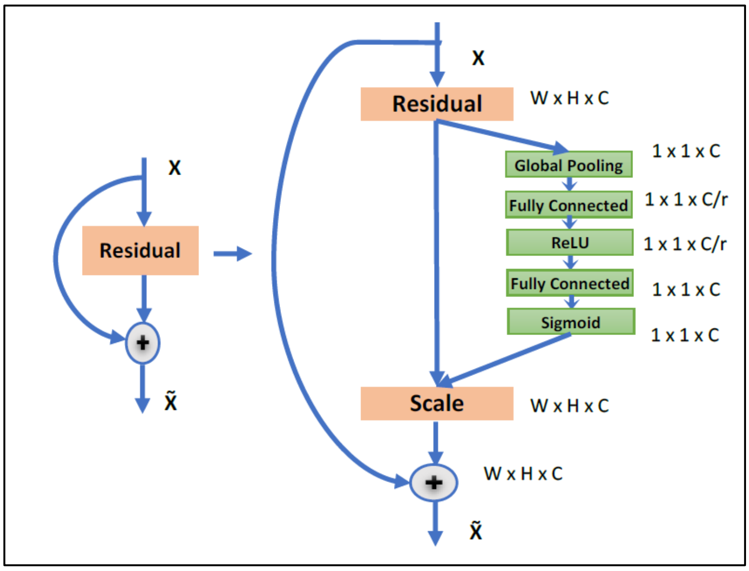

Figure 7. Block illustration of residual module.

C. Feature fusion: selection technique

In order to construct a single-dimensional feature vector, we integrated the features from ResNet50 FeatResNet and AlexNet CNN (i.e., FeatAlexNet). Before performing classification in our suggested model, both feature sets were concatenated. As a result, we got Equstion (3).

$$Feat_{DeepHybrid} = conc\,[Feat_{AlexNet}, Feat_{ResNet}] \quad (3)$$

Using SVM-RBF, the final fused feature $Feat_{DeepHybrid}$ was employed for two-class classification. The next section provides more information on the SVM-RBF model[10,20].

D. SVM-based two class classification

SVM is one of the most commonly used ML methods for categorising patterns. Due to its computational efficiency and resilience, it is perfect for classification tasks including text categorization, target recognition, picture processing, etc. SVM functions as a non-probabilistic binary classifier by learning from the input patterns because it is a supervised learning concept. By classifying the inputs using a structural risk reduction paradigm, it lowers the generalisation error over the unknowable scenarios. This SVM is a subset of the training set that retrieves the values of the so-called hyper-place boundary between two classes with differing characteristics or patterns. To accomplish two-class categorization, we used Equation (4).

$$Y' = w \times \phi(x) + b \tag{4}$$

The non linear transform is stated in Equation (4), where the focus is placed on locating the appropriate weight w and bias value b. By incrementally lowering the regression risk Equation (5) in Equation (4), Y' is calculated.

$$R_{reg}\,(Y') = C \times \sum_{i=0}^{t} \gamma\,(Y' - Y_i) + 1/2 \times \text{"}w\text{"}^2 \tag{5}$$

In Equation (5), C specifies the penalty factor and the cost function, respectively. Using Equation (6), the weight values are determined.

$$w = \sum_{j=1}^{t} (\alpha_j - \alpha^*)\; \phi(x_j) \tag{6}$$

It should be noted that in the aforementioned equation, the terms and each state a relaxation factor, also known as a Lagrange multiplier, which is always chosen as non-zero. The final output of SVM be:

$$\begin{aligned} Y' &= \sum_{j=1}^{l} (\alpha_j - \alpha^*_1)\phi(x_j) * \phi(x) + b \\ &= \sum_{j=1}^{l} (\alpha_j - \alpha^*_1) * K(x_j, x) + b \end{aligned} \tag{7}$$

It should be noted that in the aforementioned equation, the terms each state a relaxation factor, also known as a Lagrange multiplier, which is always chosen as non-zero. The final results of SVM is (x_j, x), which displays the kernel function in Equation (7). The three main kernel functions are linear, polynomial, and radial basis functions in general. We used SVM in our suggested model along with various kernel functions, including linear, polynomial, and RBF. SVM was used to categorise each test input or breast mammography picture as benign or malignant. The next sections look at the overall simulation results and their implications[29,30].

In **Figure 8**, the rows show the projected class (output class), the columns the actual cancer detection class (target class), and the columns the classification models for the features using DNN + AlexNet classification. Both the right and wrong classifications apply to maroon and orange diagonals. While the bottom row displays actual classes, the right column displays anticipated classes.

The confusion matrix for the features using the DNN + VGG classifier is shown in **Figure 9**, where columns correspond to the actual cancer detection class and rows to the classification outcomes (outlet class). The diagonal maroon and orange show whether they have been correctly or incorrectly classified. The right-hand column for each projected class shows its performance, while the matching row at the bottom shows the outcomes for the actual class.

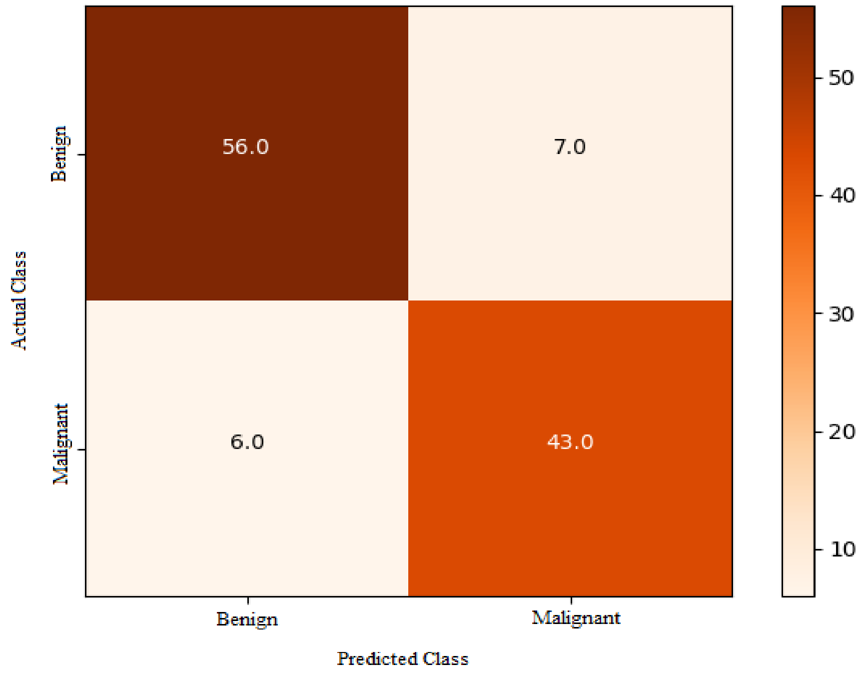

Figure 8. Confusion matrix for DNN + AlexNet.

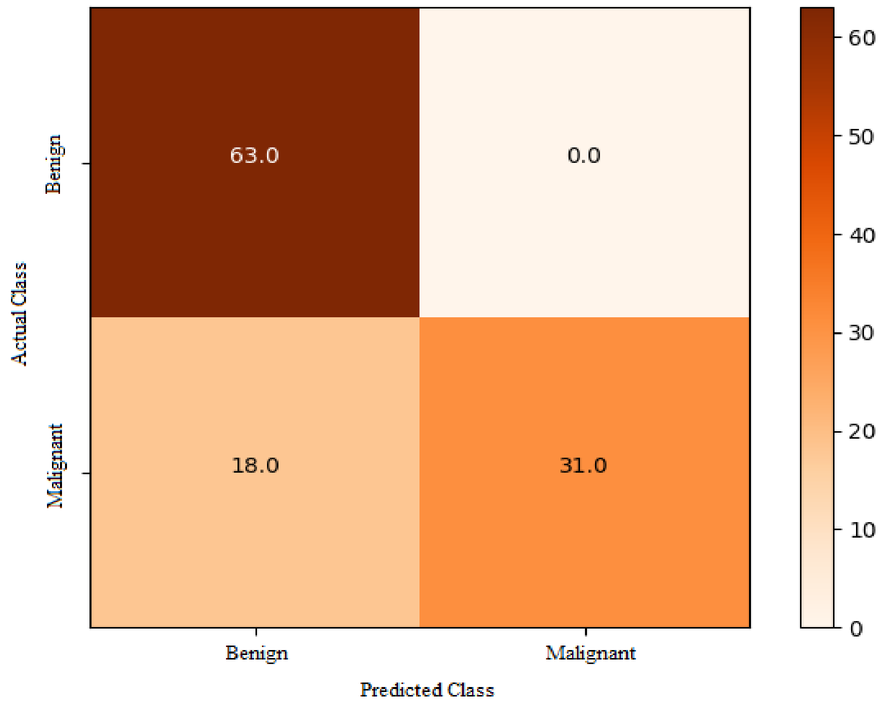

Figure 9. Confusion matrix for DNN + VGG.

The matrix for the characteristics used by the DNN + ResNet50 classification is shown in **Figure 10**, where the rows represent the predicted class (outlet class) and the sides represent the actual category (targeted class) of the cancer detection data. The longitudinal maroon and orange show whether or not they have been correctly or incorrectly classified. The bottom row displays the actual classes, while the right column displays the projected classes.

The confusion matrix for the feature using DNN + ResNet101 classification is shown in **Figure 11**. Columns are used to display both the predicted class (the result class) and the true class (the intended class). The diagonal maroon and orange colours illustrate which classifications are correct and incorrect. Predicted courses are shown in the right column, and classroom effectiveness is shown in the bottom row. Additionally, the second picture class is known as the breast cancer picture class because our model correctly identifies 1277 images from it, whereas only 252 images from the regular picture class have labels attached.

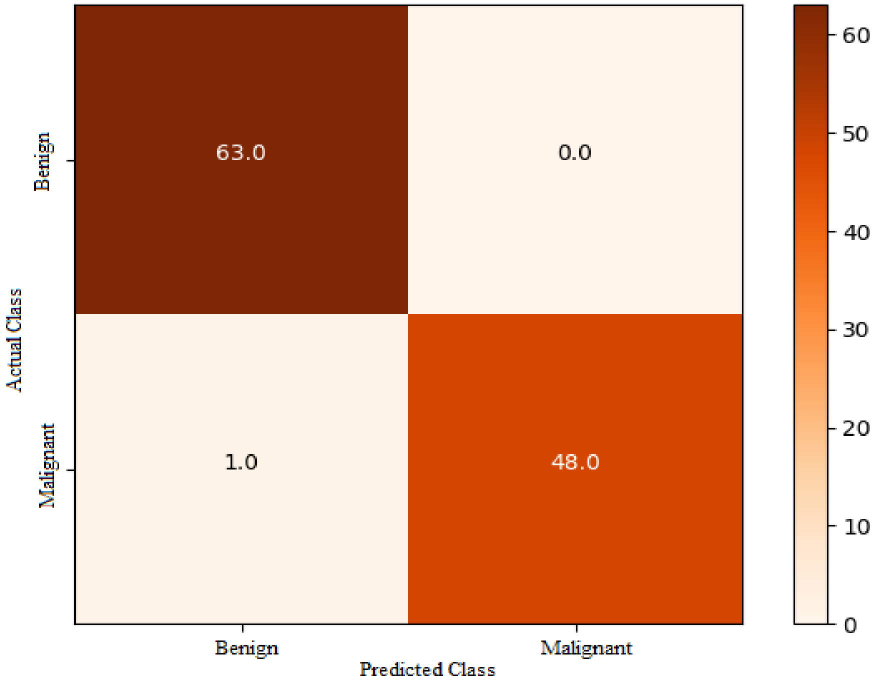

Figure 10. Confusion matrix for DNN + ResNet50.

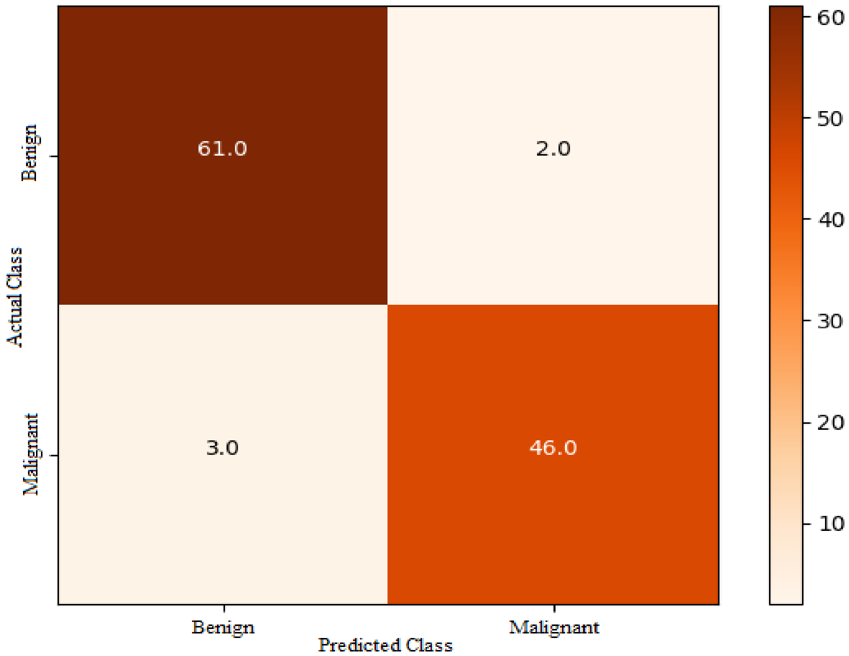

Figure 11. Confusion matrix for DNN + ResNet101.

The deep DNN-based ResNet101 framework is proposed for automatically classifying breast cancer. We think that the suggested approach might be a useful resource for clinicians to classify breast tumors. This study provides a hybrid depth-based machine-learning strategy for breast cancer tissue recognition and characterization. Instead of using only one method, the proposed framework incorporates DL and ML methods to maximize efficacy. AlexNet and ResNet101 are used to retrieve feature representations. This research specifically suggested that the deliberate fusion of deep characteristics might facilitate the more precise acquisition of breast cancer tissue pattern learning and subsequent classification. In this connection, characteristics were obtained from AlexNet and shorted ResNet101, the former containing multiple convolutional layers and 3 fully linked layers and the latter as a simulation exercise. The fusion characteristic was learned utilizing SVMs and RBF to identify benign or malignant mammograms. Both a scalar metric and a visual method are used in this study to assess resilience. It could also be useful for other uses, such that the classification of brain tumors, liver lesions, etc.[30].

E. ROC-receiver operating characteristic curve

It is described as a line with 450 points and an AUC of 0.5. Since this model's AUC is higher than the AUC of a random line, it is regarded as being superior. The curve then creates a right-angled triangular from the model with the highest AUC, which is 1, and from this point. The model misclassifies at $Y = 0$ if the randomly generated line is in the bottom left corner. In error, the random line appeared at $Y = 1$ in the upper right corner when it should not have. A comparison of various classification models is shown in **Table 1**. The classifier is used to perform two separate features[30–32].

F. Hybridized learning models to improve breast cancer detection on mammography

The efficiency of these algorithms for categorising data, however, ultimately depends on the characteristics that are extracted and used. However, in the real world, accurate classification requires a particular pre-trained model. The vast majority of deep learning models were created using this dataset to maximise their learning potential. It makes categorization dependent on prior knowledge of the characteristics. However, in reality, a patient can only have so many mammography or biopsy histopathological tissue images. This may lead to false positives or false negatives when a secondary pre-trained version is used in conjunction with the patient's own (primary, let's say) collection of limited images. In this study, a very trustworthy deep hybrid machine learning model (AlexResNet+) for categorising breast cancer tissues is developed while taking into account the aforementioned key conclusions. The DL methods AlexNet, CNN, and ResNet to get the appropriate collection of top characteristics for further classification. To recover the hybrid features, we employed SVM with an RBF kernel in a two-class classification. By utilising a 10-fold cross-validation-based classification, our recommended AlexResNet + model achieves an accuracy of 95.87%, a precision of 0.9760, a sensitivity of 1.0, a specificity of 0.9621, an F-Measure of 0.9878, and an AUC of 0.960. The whole suggested model was built on the matlab 2019b platform, and simulation results using the DDSM dataset showed that it outperforms the majority of existing systems for classifying breast cancer tissues[33].

Researchers found that combining these two architectural techniques improved mammographic detection accuracy. For instance, one study used AlexNet and ResNet to categorise breast tumours as benign or cancerous. According to the statistics, the combined design outperformed either AlexNet or ResNet by itself, with an accuracy of 93.6%. But I combined several techniques in my research, including AlexResNet + 95.44 for the SVM-polynomial intra-model performance assessment and AlexResNet + 95.87 for the SVM-RBF intra-model performance assessment.

Table 2 reveals that AlexResNet + characteristics have the best overall results, particularly in terms of accuracy (92.31%), precision (0.9411), sensitivity (1.000), specificity (0.8235), and F-score or F-Measure (0.9696). However, ResNet50 supported deep features also outperformed the AlexNet-CNN feature. Notably, the findings reported above used an SVM classifier that learned using a linear kernel function. The AlexResNet + features also performed better with SVM-polynomial classification, as shown in **Table 3**, with accuracy of 95.45%, precision 0.97, sensitivity 1.000, specificity 0.97 and F-Measure of 0.98. The proposed AlexResNet+

feature is more effective at identifying breast cancer tissue and making related diagnoses. In our suggested model, SVM-RBF, which has been shown acceptable for multiple classification tasks, performs better (**Table 4**). The suggested AlexResNet+ feature-based model obtains the maximum classification accuracy (95.87%), precision (0.9760), sensitivity (1.000), specificity (0.9621), and F-Measure, according to the simulation results using SVM-RBF classifier (0.9878). This finding confirms the potential of AlexResNet+ characteristics for identifying and categorizing chest cancerous tissue. We achieve the following by taking into account the greatest performance for the various classifiers (in combination with the various characteristics) (**Table 3**) with our suggested model[33].

Table 2. Intra-model performance assessment with SVM-linear.

Deep features	Performance variables				
	Accuracy (%)	Precision	Recall (sensitivity)	F-Measure	Specificity
AlexNet-CNN	89.75	0.91	1.01	0.95	0.77
ResNet50	92.28	0.92	1.01	0.93	0.83
AlexResNet+	92.32	0.95	1.01	0.97	0.83

Table 3. Intra-model performance assessment with SVM-polynomial.

Deep features	Performance variables				
	Accuracy (%)	Precision	Recall (sensitivity)	F-Measure	Specificity
AlexNet-CNN	89.5	0.92	0.824	0.87	0.826
ResNet50	93.3	0.96	0.95	0.96	0.828
AlexResNet+	95.5	0.96	1.01	0.98	0.95

Table 4. Intra-model performance assessment with SVM-RBF.

Deep features	Performance variables				
	Accuracy (%)	Precision	Recall (sensitivity)	F-Measure	Specificity
AlexNet-CNN	89.71	0.924	0.955	0.95	0.89
ResNet50	92.11	0.932	0.956	0.95	0.89
AlexResNet+	95.88	0.977	1.01	0.99	0.97

According to the data (**Table 5**), SVM-RBF outperforms the other two SVM classifier variations, with accuracy scores of 95.87%, 0.9760 precision, 1.000 recall or sensitivities, 0.9621 specificity, and 0.9878 F-Measure. Therefore, for this study endeavor, it was recommended to use an AlexResNet+ features aided SVM-RBF classifier for the detection and classification of breast cancer tissue. To get the best moment and allied modeling as a research work, we evaluated our proposed framework to alternative methodologies. The next part provides a thorough analysis of the various current techniques and a performance compared with our suggested model.

Table 6 shows a comparison of several categorization models. Two distinct features, are performed using the classifier.

Table 5. Classifier-centric performance assessment with AlexResNet+ feature.

Deep features	Performance with AlexResNet+ features				
	Accuracy (%)	Precision	Recall (sensitivity)	F-Measure	Specificity
SVM-linear	92.31	0.9411	1.000	0.9696	0.8235
SVM-polynomial	95.44	0.9565	1.000	0.9777	0.9412
SVM-RBF	95.87	0.9760	1.000	0.9878	0.9621

Table 6. Evaluation of different methods classifier.

Methods	Accuracy	Precision	Recall	F1-score
DNN + AlexNet	83.94%	88.90%	81.63%	82.6%
DNN + VGG	88.40%	88.17%	88.33%	88.24%
DNN + ResNet50	91.97%	92.20%	91.6%	91.78%
DNN + ResNet101	95.55%	95.58%	95.36%	95.46%

4. Simulation results in graphics

The steady growth changes depending on the value of *k*, as shown in **Figure 12a**. The RF and Pearson approaches appear to offer the most reliable results, SVM stability RFEs are quite subpar for small values of *k*. Only once can the techniques be used to extract the most important characteristics. Combining the rankings to obtain a more accurate one is a great option. Wrapper approaches are also very unpredictable. We use MDS to compare feature selections. The tests we performed can be defined as a collection of 46 data because we used six separate procedures and launched each method seven times. This describes a space with 124 dimensions.

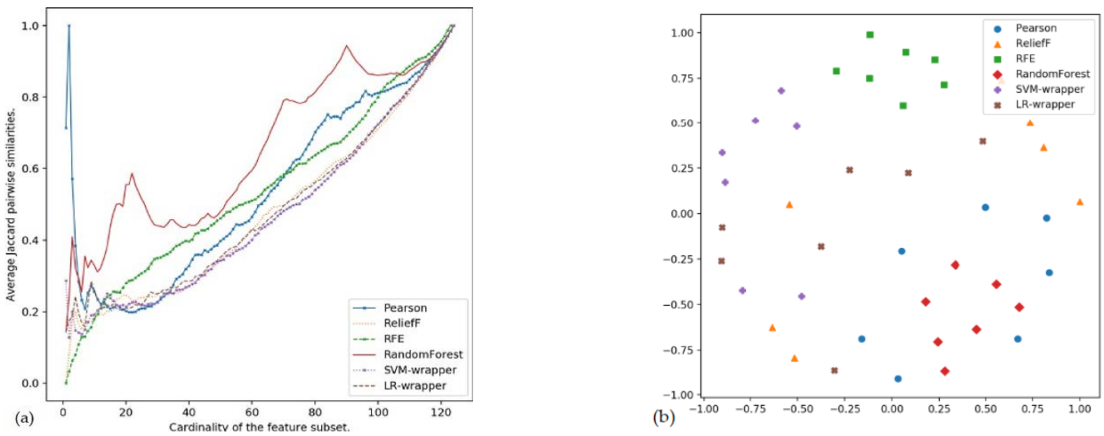

Figure 12. Feature selection: **(a)** the Jaccard value of the retrieved feature; **(b)** the MDS plot of the characteristic.

These locations are projected in two dimensions using the MDS. Spearman's rank correlation is used to calculate the distance between the locations, and total squared divergences are used to normalize the pressure requirements. Each and every algorithmic output (x, y) is then given a pair of places using this two-dimensional representation. **Figure 12b** shows how similar the feature selectors are to one another. It should be noted that the results from SVM wrapper, SVM RFE, and RF are more tightly packed in terms of stability than those from pearson, Relief F, and LR wrapper. It's vital to consider both the approaches' stability and their accuracy in class prediction. This is crucial because professionals require information on the most critical risk variables and protective factors rather than merely data on the most reliable techniques[33].

5. Discussion

The empirical correlation of all DNN characteristics with the AlexNet, VGG, ResNet50, and ResNet101 algorithms is shown in **Figure 13**.

Breast tumour mammo pictures are automatically segmented and categorised for tumour prediction using a "DNN + AlexNet + ResNet101" integrated model. Furthermore, experimental findings show that the proposed method can significantly outperform the other recently developed competitive breast tumour classification methods in terms of overall accuracy, precision, and specificity. As a result, the proposed method may be a helpful tool for doctors to classify breast cancers. It might also be helpful for other purposes, such as the classification of liver lesions or brain tumours, etc. Future improvements to the proposed model could include incorporating three-dimensional data provided by any dimensional inputs as well as outputs and covering a wider range of classes.

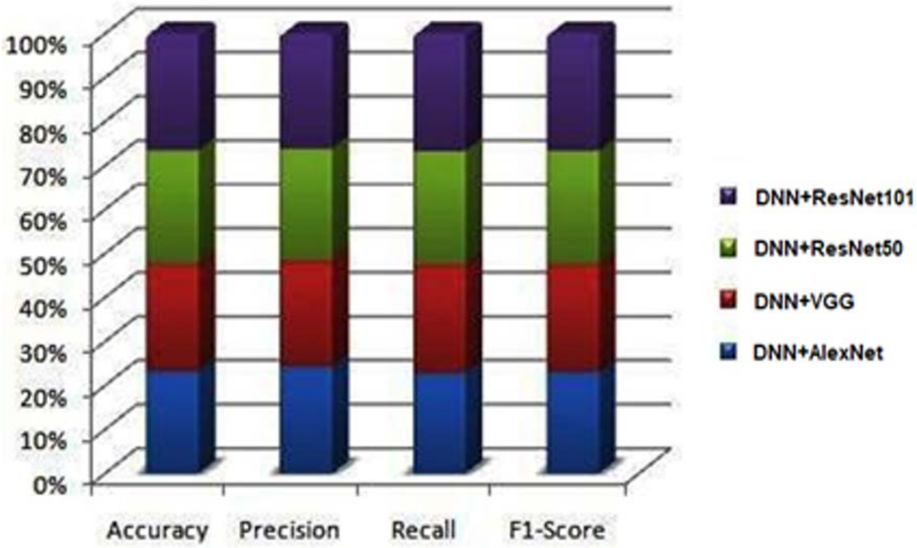

Figure 13. Overall evaluation of the models.

6. Conclusion

In the early work, the top-five accuracy of AlexNet, VGG, and ResNet50, together with accurately and automatically formed areas, are all estimated to have about 60 M parameters, but there may be a 10% variation between them. The MLO View was helpful in making this happen. However, learning ResNet-150 involves performing many calculations (roughly ten times more than AlexNet), which suggests that more study time and effort are required. VGGNet not only provides a greater variety of variables and FLOP but is also less accurate than ResNet-150. Training time for inaccurate VGG-Nets is longer. Learning an AlexNet and training conception both require about the same amount of time. The high degree of accuracy of the memory requirements is much lower (or about 9%). With remarkable results and model parameters, ResNet resolves degradation. All previous incidents would be resolved by ResNet50, which would improve FP results for mammogram identification. For discriminating between normal and pathological regions in mammography, ResNet50 is trustworthy and secure since efficiency increases after FP makes a decision on its own. A deep DNN-based ResNet101 architecture is suggested in the study that follows for automatically classifying breast cancer. We believe that the offered method could be a helpful tool for clinicians to classify breast tumours.

This work offers a hybrid depth-based ML technique for identifying and characterizing BS tissue. To increase effectiveness, the suggested framework combines DL and ML algorithms rather than employing only one. The feature representations are retrieved using ResNet101 and AlexNet. This study in particular made the case that the deliberate merger of deep traits might make learning breast cancer tissue patterning and subsequent categorization more accurate. In this regard, traits were taken from ResNet101 and AlexNet, the latter serving as a simulation exercise while the former contained numerous convolutional layers and three fully linked layers. The fusion characteristic was trained to discriminate between benign and malignant mammograms using SVMs and RBF. Resilience is assessed in this study using both a scalar metric and a visual method. It might be useful for other things as well, like categorising brain cancers, liver lesions, and other things.

Author contributions

Conceptualization, SSH; methodology, SSH; software, SSH; validation, HT; data curation, SSH; writing—original draft preparation, HT; writing—review and editing, HT; visualization, HT; supervision, DVC; project administration, DVC. All authors have read and agreed to the published version of the manuscript.

Conflict of interest

The authors declare no conflict of interest.

Data availability statement

The dataset used in this work is publicly available (CBIS-DDSM).

References

1. Ali I, Wani WA, Saleem K. Cancer scenario in India with future perspectives. *Cancer Therapy* 2011; 8(8): 56–70.
2. Urbanowicz RJ, Meeker M, La Cava W, et al. Relief-based feature selection: Introduction and review. *Journal of Biomedical Informatics* 2018; 85: 189–203. doi: 10.1016/j.jbi.2018.07.014
3. Siegel RL, Miller KD, Jemal A. Cancer statistics, 2017. *CA: A Cancer Journal for Clinicians* 2017; 67(1): 7–30. doi: 10.3322/caac.21387
4. Roy K, Banik D, Bhattacharjee D, Nasipuri M. Patch-based system for classification of breast histology images using deep learning. *Computerized Medical Imaging and Graphics* 2019; 71: 90–103. doi: 10.1016/j.compmedimag.2018.11.003
5. Shruthishree SH, Tiwari H. A review paper on medical image processing. *International Journal of Research-Granthaalayah* 2017; 5(4): 21–29. doi: 10.29121/granthaalayah.v5.i4RACSIT.2017.3344
6. He L, Long LR, Antani S, Thoma GR. Histology image analysis for carcinoma detection and grading. *Computer Methods and Programs in Biomedicine* 2012; 107(3): 538–556. doi: 10.1016/j.cmpb.2011.12.007
7. Veta M, Pluim JPW, Van Diest PJ, Viergever MA. Breast cancer histopathology image analysis: A review. *IEEE Transactions on Bio-Medical Engineering* 2014; 61(5): 1400–1411. doi: 10.1109/TBME.2014.2303852
8. Ferlay J, Colombet M, Soerjomataram I, et al. Cancer incidence and mortality patterns in Europe: Estimates for 40 countries and 25 major cancers in 2018. *European Journal of Cancer* 2018; 103: 356–387. doi: 10.1016/j.ejca.2018.07.005
9. Zhi W, Yueng HWF, Chen Z, et al. Using transfer learning with convolutional neural networks to diagnose breast cancer from histopathological images. In: Proceedings of the 24th International Conference On Neural Information Processing; 14–18 November 2017; Guangzhou, China. pp. 669–676.
10. Shruthishree SH, Tiwari H, Devaraj Verma C. Resnet deep learning technique to improve breast cancer detection on screening mammography. *Journal of Critical Reviews* 2023; 7(19): 8250–8271. doi: 10.31838/jcr.07.19.932
11. Srivastava A, Kumar VV, Mahesh TR, Vivek V. Automated prediction of liver disease using machine learning (ML) algorithms. In: Proceedings of 2022 Second International Conference on Advances in Electrical, Computing, Communication and Sustainable Technologies (ICAECT); 21–22 April 2022; Bhilai, India. doi: 10.1109/ICAECT54875.2022.9808059
12. Bhuiyan MNQ, Shamsujjoha M, Ripon SH, et al. Transfer learning and supervised classifier based prediction model for breast cancer. In: *Big Data Analytics for Intelligent Healthcare Management*. Academic Press; 2019. pp. 59–86.

13. Kharya S. Using data mining techniques for diagnosis and prognosis of cancer disease. *International Journal of Computer Science, Engineering and Information Technology (IJCSEIT)* 2012; 2(2): 55–66. doi: 10.5121/ijcseit.2012.2206
14. Mathiyalagan R, Pamela Vinitha Eric, review on intrusion detection system based methods on knowledge discovery data (kdd) dataset. *Journal of Critical Reviews* 2020; 7(10): 3023–3029.
15. Fenton JJ, Taplin SH, Carney PA, et al. Influence of computer-aided detection on performance of screening mammography. *New England Journal of Medicine* 2007; 356(14): 1399–1409. doi: 10.1056/NEJMoa066099
16. Cole EB, Zhang Z, Marques HS, et al. Impact of computer-aided detection systems on radiologist accuracy with digital mammography. *American Journal of Roentgenology* 2014; 203(4): 909–916. doi: 10.2214/AJR.12.10187
17. Lehman CD, Wellman RD, Buist DSM, et al. Diagnostic accuracy of digital screening mammography with and without computer-aided detection. *JAMA Internal Medicine* 2015; 175(11): 1828–1837. doi: 10.1001/jamainternmed.2015.5231
18. Madhuri GS, Mahesh TR, Vivek V. A novel approach for automatic brain tumor detection using machine learning algorithms. In: *Big Data Management in Sensing*. River Publishers; 2021. pp. 87–101.
19. Aboutalib SS, Mohamed AA, Berg WA, et al. Deep learning to distinguish recalled but benign mammography images in breast cancer screening. *Clinical Cancer Research* 2018; 24(23): 5902–5909. doi: 10.1158/1078-0432.CCR-18-1115
20. Shruthishree SH, Harshvardhan T, Devaraj V. Integrated IoT-based healthcare system for the early detection of breast cancer using intelligent diagnostic system. *Journal of Machine and Computing* 2023; 27–37. doi: 10.53759/7669/jmc202303004
21. Khan S, Islam N, Jan Z, et al. A novel deep learning based framework for the detection and classification of breast cancer using transfer learning. *Pattern Recognition Letters* 2019; 125(1): 1–6. doi: 10.1016/j.patrec.2019.03.022
22. Spanhol FA, Oliveira LS, Petitjean C, Heutte L. Breast cancer histopathological image classification using convolutional neural networks. In: Proceedings of 2016 International Joint Conference On Neural Networks; 24–29 July 2016; Vancouver, BC, Canada. pp. 2560–2567.
23. Devarajan D, Alex DS, Mahesh TR, et al. Cervical cancer diagnosis using intelligent living behavior of artificial jellyfish optimized with artificial neural network. *IEEE Access* 2022; 10: 126957–126968. doi: 10.1109/ACCESS.2022.3221451
24. Li Y, Wu J, Wu Q. Classification of breast cancer histology images using multi-size and discriminative patches based on deep learning. *IEEE Access* 2019; 7: 21400–21408. doi: 10.1109/ACCESS.2019.2898044
25. Cascianelli S, Bello-Cerezo R, Bianconi F, et al. Dimensionality reduction strategies for CNN-based classification of histopathological images. In: *International Conference on Intelligent Interactive Multimedia Systems and Services*. Springer; 2019. pp. 21–30.
26. Mahesh TR, Kaladevi AC, Balajee JM, et al. An efficient ensemble method using k-fold cross validation for the early detection of benign and malignant breast cancer. *International Journal of Integrated Engineering* 2022; 14(7): 204–216.
27. Bhattacharjee S, Mukherjee J, Nag S, et al. Review on histopathological slide analysis using digital microscopy. *International Journal of Advanced Science and Technology* 2014; 62: 65–96. doi: 10.14257/ijast.2014.62.06
28. Ramakrishna MT, Venkatesan VK, Izonin I, et al. Homogeneous Adaboost Ensemble machine learning algorithms with reduced entropy on balanced data. *Entropy* 2023; 25(2): 245. doi: 10.3390/e25020245
29. Bergmeir C, Silvente MG, Benítez JM. Segmentation of cervical cell nuclei in high-resolution microscopic images: A new algorithm and a web-based software framework. *Computer Methods and Programs in Biomedicine* 2012; 107(3): 497–512. doi: 10.1016/j.cmpb.2011.09.017
30. Haralick RM, Shanmugam K, Dinstein I. Textural features for image classification. *IEEE Transactions on Systems Man and Cybernetics* 1973; 3(6): 610–621.
31. Hang PW, Lai YH. Effective segmentation and classification for HCC biopsy images. *Pattern Recognition* 2010; 43(4): 1550–1563. doi: 10.1016/j.patcog.2009.10.014
32. Landini G, Randell DA, Breckon TP, Han JW. Morphologic characterization of cell neighborhoods in neoplastic and preneoplastic epithelium. *Analytical and Quantitative Cytology and Histology* 2010; 32(1): 30–38. doi: 10.1165/rcmb.2008-0488OC
33. Devaraj VC, Shruthishree SH, Harshvardhan T. AlexResNet+: A deep hybrid featured machine learning model for breast cancer tissue classification. *Turkish Journal of Computer and Mathematics Education (TURCOMAT)* 2021; 12(6): 2420–2438. doi: 10.17762/turcomat.v12i6.5686